In-situ preparation of nanocomposite comprising graphene and α-Fe_2O_3 nanospindles for photo-degradation of antibiotic under visible light

Komal Arora,[a] Sekar Karthikeyan,[b] Bilal Ahmad Shiekh,[a] Manvir Kaur,[a] Harjinder Singh,[a] Gopala Ram Bhadu,[c] Tejwant Singh Kang,*[,a]

[a] *Department of Chemistry, UGC-centre for Advance Studies–II, Guru Nanak Dev University, Amritsar, 143005, India.*

[b]*Department of Earth Resources Engineering, Faculty of Engineering, Kyushu University, 744 Motooka, Nishiku, Fukuoka 819-0395, Japan.*

[c]*Analytical and Environmental Science Division and Centralized Instrument Facility, CSIR-Central Salt and Marine Chemicals Research Institute, G. B. Marg, Bhavnagar-364002, Gujarat*

Supporting Information

**To whom correspondence should be addressed: E-mail*: tejwantsinghkang@gmail.com; tejwant.chem@gmail.com Tel: +91-183-2258802-Ext-3207

1. Annexure S1

1.1. Materials

Graphite (+100 mesh, product no. 332461) and Sulfamethoxazole (98%) were purchased from Sigma Aldrich and were used as received. Ferric chloride hexahydrate ($FeCl_3 \cdot 6H_2O$, 98%), 1-Methylimidazole (> 99%), 1–Chlorohexadecane (> 99%), Dichloromethane (AR grade), Diethyl ether (AR grade), Hexane (AR grade), and Ethyl acetate (AR grade) were purchased from SD Fine-Chem. Ltd., India.

1.2. Exfoliation and Characterization of exfoliated Graphene Sheets

An aqueous solutions of $[C_{16}mim][FeCl_4]$, at different concentrations (0.1 mmol L^{-1} to 100 mmol L^{-1}), in the presence of 12.5 mg ml^{-1} of pristine graphite, were sonicated for 1 hour using bath sonicator (Citizon CUB2.5, Power 50W, Frequency 40 KHz). The used $[C_{16}mim][FeCl_4]$ was synthesized and characterised using method reported in literature.[1a-c] The surface active nature of prepared IL, $[C_{16}mim][FeCl_4]$ has been checked employing surface tension measurements (Kyowa Dyne master (DY-500) tensiometer by Du Noüy Ring Method). Thus, formed suspensions of graphene in aqueous solution of $[C_{16}mim][FeCl_4]$ were centrifuged at 1000 rpm for 1 hour to remove unexfoliated graphite precipitated below and the graphene sheets present in dark supernatant was recovered carefully. The concentration of exfoliated graphene flakes in aqueous solutions has been determined using simple gravimetric analysis.[2] UV-visible absorption spectra of thus obtained supernatant were measured using UV-Vis spectrophotometer (Cary 5000 UV-Vis-NIR) in the wavelength range of 500-800 nm using quartz cuvette having path length of 1 cm. X-ray diffraction patterns of graphite flakes and exfoliated graphene sheets were acquired on a Rigaku Xpert Pro X-ray diffractometer having a Cu-target in the 2θ range of 5-80° with step size of 0.02°. Raman spectra of graphite flakes and exfoliated graphene sheets after washing the graphene sheets by double distilled water and ethanol followed by air drying for 24 h were recorded on Renishaw Raman Spectrophotometer

in the range of 3500-300 cm^{-1} using Ar-ion laser at a wavelength of 514 nm. Zeta (ζ)-potential measurements were performed using light scattering apparatus (Zeta-sizer, nanoseries, nano-ZS), Malvern Instruments, equipped with a built-in temperature controller having an accuracy of ±0.1 K at a scattering angle of 173° using dip cell (ZEN-212). ^{1}H NMR and 2D ^{1}H−^{1}H NOESY experiments were performed on a Brüker Ascend 500 spectrometer (AVANCE III HD console) with water suppression in a 10% D_2O−90% H_2O mixture. Phase sensitive 2D ^{1}H−^{1}H NOESY experiment was recorded with 32 number of scans and mixing time of 500 ms. X-ray photoelectron spectroscopy (XPS) was performed on a Kratos Axis His spectrometer with monochromated Al Kα X-ray source operated at 90 W with magnetic focusing and a charge neutraliser. Spectra were fitted using Casa XPS version 2.3.16, with energy referencing to adventitious carbon at 284.6 eV. The size, morphology and lattice structure of exfoliated graphene sheets were investigated by JEM-2100 transmission electron microscope (TEM) at a working voltage of 200 kV. For the TEM measurement, the obtained powder was dispersed in ethanol sonication in a bath sonicator for 10 minutes. A drop of dispersion was placed on the carbon coated grid (300 mesh) and the samples were dried at room temperature for 24 hours before the measurements. Atomic force microscopy (AFM) was recorded using tapping mode on Anton Parr Tosca 400 Series. Samples were drop casted on freshly prepared mica surface and air dried for 24hours before measurement.

1.3. Preparation of α-Fe_2O_3@G nanocomposite (NCs)

The concentration of $[C_{16}mim][FeCl_4]$ containing exfoliated graphene sheets has been increased from 5 mmol $L^{-1}$to 50 mmol $L^{-1}$for the preparation of α-Fe_2O_3 nanoparticles (NPs), as low concentration of $[C_{16}mim][FeCl_4]$ does not results in formation of NPs. An aqueous dispersion of graphene in 50 mmol $L^{-1}$of $[C_{16}mim][FeCl_4]$ was micowaved (Anton Parr Monowave 200 having power of 850W) for 30 min at temperature of 130 ^oC with stirring at 600 rpm. After cooling to room temperature, the obtained products were washed several times

with distilled water and methanol to remove the residual [C_{16}mim][$FeCl_4$], if any. The prepared material is air dried for 24 h and has been abbreviated as α-Fe_2O_3@G. The α-Fe_2O_3 NPs has also been prepared by following same procedure in the absence of graphene sheets and abbreviated as α-Fe_2O_3.

1.4. Characterization of α-Fe_2O_3@G NCs

The structural characterization of prepared composite has been done using XRD, Raman, XPS, TEM and UV-Visible spectroscopy by employing same method and same machines used for characterization of graphene sheets. Photoluminescence spectra of prepared NCs were recorded on a Horiba Fluorolog spectrophotometer using the excitation wavelength of 320 nm employing an excitation and emission slit width of 1 each. The measurements were made using a quartz cuvette of path length 1 cm in the wavelength range of 360-460 nm. For both UV-Vis and photoluminescence measurements, spectra were recorded by dispersing equal amount of α-Fe_2O_3@G nanocomposite and α-Fe_2O_3 in distilled water as solvent. The magnetic properties of prepared nanocomposite have been investigated using Microsense EV-90 vibrating sample magnetometer (VSM) in the applied magnetic field of -20 to +20 kOe at room temperature. FT-IR spectra of prepared NCs and their counterparts have been recorded on recorded on Agilent Cary 630 FTIR spectrometer in the range of 400-3000 cm^{-1}.For thermogravimetric analysis (TGA) measurements, the prepared α-Fe_2O_3@G nanocomposite after washing with distilled water and ethanol followed by air drying for 24 hours, were carried out using HITACHI STA7200 thermal analysis system at a scan rate of 10 ^oC/min in temperature range from 25 ^oC to 850 ^oC.

1.5. Sulfamethoxazole (SMX) photodegradation experiment

20 mg of photocatalysts were dispersed in 50 mL of SMX (0.01184 mM) in a 250 mL photoreactor and then sonicated 10 min for complete dispersion. Prior to light illumination, the

mixture was stirred in dark to reach adsorption-desorption equilibrium. After adsorption, 1mL sample was taken for HPLC analysis, and then sample was continuously stirred under visible light irradiation (cut-off filter above 420 nm; temperature maintained 25° C, stirring speed RPM maintained 500; light intensity 1.82 mV/cm^2, effective irradiation area was 4.5 cm and distance from light source to sample is 14.9 cm). Samples were collected at different time intervals using CPO20AN filter for all samples including initial sample.

1.6. HPLC calibration

SMX was analysed using a high performance liquid chromatography (HPLC) system (JASCO UV plus 2075, Japan) coupled with UV/Vis detector selected at λ = 254 nm and a Shodex C18M 4E analytical column (4.6 I.D × 250mm), separation factor (α_1 = 2.42 and α_2 = 1.47) with a constant temperature of 25 °C and pressure maximum 20 M Pa, pressure minimum 0.2 MPa. The eluent consists of 60:10:30 (*v*/*v*) acetonitrile: water: formic acid (25mM) (TCI, Japan) with a flow rate of 0.6 mL/min.

1.7. Apparent quantum efficiency (AQE) determination

$$Apparent quantum efficiency\ (\%) = \frac{Mols\ of\ reacted\ electrons\ per\ unit\ time}{Mols\ of\ incident\ photons\ per\ unit\ time} \times 100 \quad \text{(S1)}$$

$$\text{Mols incident photons per unit time } (N_{Einstein}) = \frac{Number\ incident\ photons\ per\ unit\ time}{N_A}$$

Number of incident photons N_p per unit time can be calculated by:

$$N_p = \frac{Intensity\ (E)}{Photon\ energy\ (Ep)} \text{ and } photonenergy\ (Ep) = \frac{hc}{\lambda} \quad \text{(S2)}$$

E = Irradiance × reactor area illuminated

$$E_p = \frac{(6.625 \times 10^{-34} J.s)(3 \times 10^{17} nm.s^{-1})}{\lambda(nm)} = \frac{19.88 \times 10^{-17}}{\lambda(nm)} = 4.73 \times 10^{-19} J$$

(S3)

$$N_p = \frac{E}{E_p} = 0.00189/4.73\times10^{-19} = 1.73\times10^{16} \text{ J} \quad \text{(S4)}$$

$$N_{Einstein} = \frac{N_p}{N_A} = 2.87\times10^{-6} \text{ mols.s}^{-1} \quad \text{(S5)}$$

1.8.Transient photocurrent and Electrochemical impedance spectroscopy (EIS) measurement

Transient photocurrent and Electrochemical impedance spectroscopy (EIS) measurement was conducted by an electrochemical instrument in 0.5 M Na_2SO_4 electrolyte solution in single compartment quartz cell. A three-electrode cell system was applied with 10 mg of samples on FTO glass as the working electrode, Pt wire as the counter electrode, and Ag/AgCl as the reference

1.9. Computational Details

In order to provide in depth insights regarding photocatalytic activity of α-Fe_2O_3@G interface, spin-polarized calculations were performed at density functional theory (DFT) level employing Perdew–Burke–Ernzerh of (PBE) exchange–correlation functional[3] with projected augmented wave (PAW) approximation[4] with 400eV energy cut off. The Brillouin zone integration was sampled using 8×8×1 Monkhorst–Pack[5] 3Γ-centered k-point mesh for all calculations. The 10^{-5} eV and 10^{-2} eV/Å convergence criteria for energy and forces, respectively were employed with lattice constants kept fixed while all atoms set free to relax during geometry optimization calculations. All the above said calculations have been performed using Vienna ab Initio Simulation Package (VASP).[6-8] To model α-Fe_2O_3/G interface, we first constructed a slab of α-Fe_2O_3 (001) containing total six atomic layers three of each oxygen and iron from the CIF file

(hematite) downloaded from materials project repositories website.[9] On top of our newly constructed slab, we inserted graphene supercell such that the lattice parameters of both the supercells become equal to each other. From this supercell, we constructed a unit cell having total 28 atoms (8 Fe, 12 O and 8 C) and lattice parameters 5.038×5.035×30.000Å.[9] A vacuum region of 20 Å was added along the z-direction to avoid unnecessary interfacial interactions.

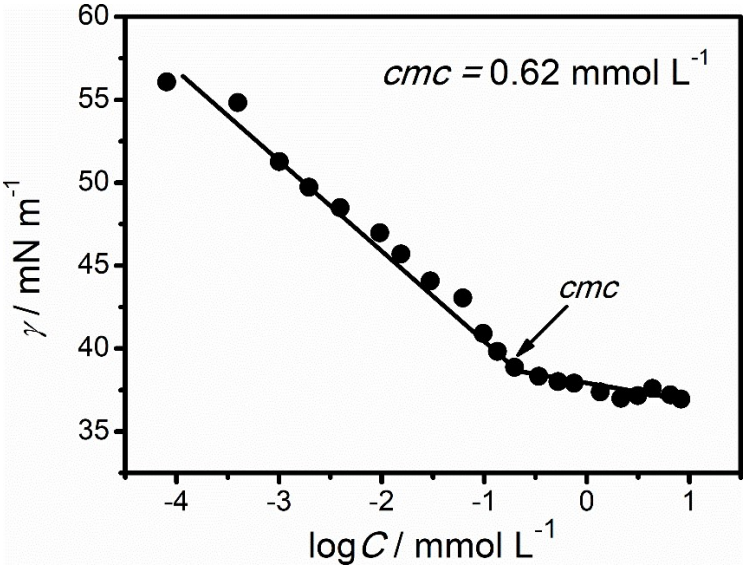

Figure S1: Surface tension (γ) profile of $[C_{16}mim][FeCl_4]$ by variation of concentration in aqueous medium at 298.15 K.

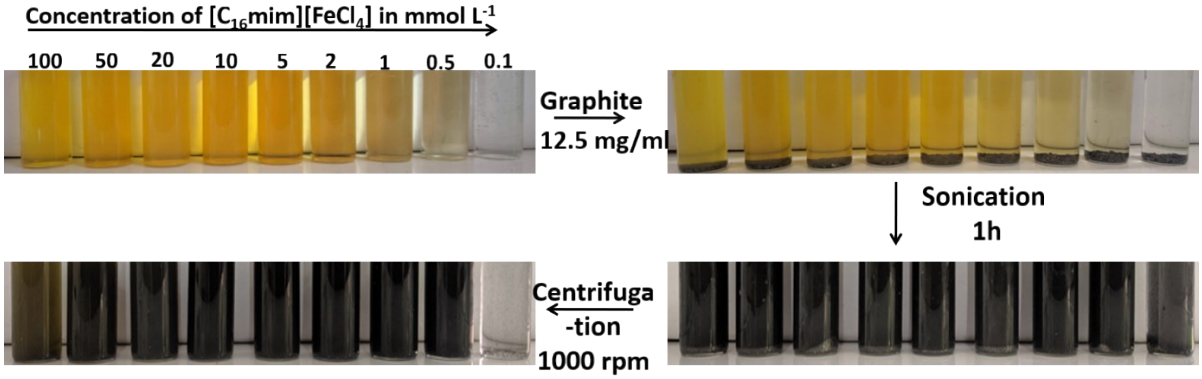

Figure S2: Photographs showing $[C_{16}mim][FeCl_4]$ mediated dispersion of graphene in nine different concentrations of aqueous solutions of $[C_{16}mim][FeCl_4]$.

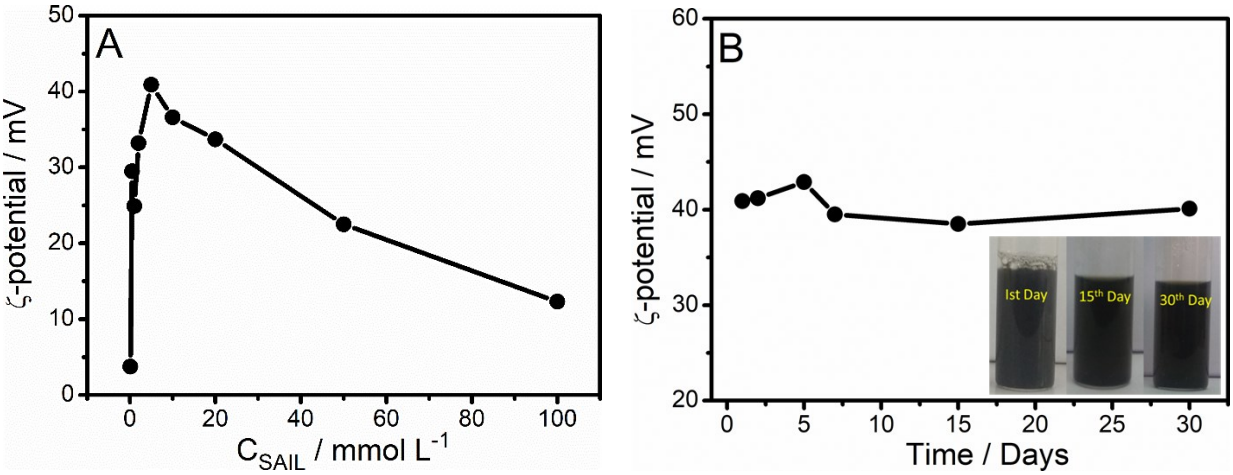

Figure S3: (A) Zeta (ζ)-potential change as a function of SAIL concentration in aqueous solution with graphene and; (B) Zeta-potential of graphene dispersion in aqueous solution of 5 mmol L^{-1} concentration of SAIL as a function of time. Inset of B visually shows the colloidal stability of exfoliated graphene sheets dispersions at $[C_{16}mim][FeCl_4]$ concentration of 5 mmol L^{-1} for a period of 30 days.

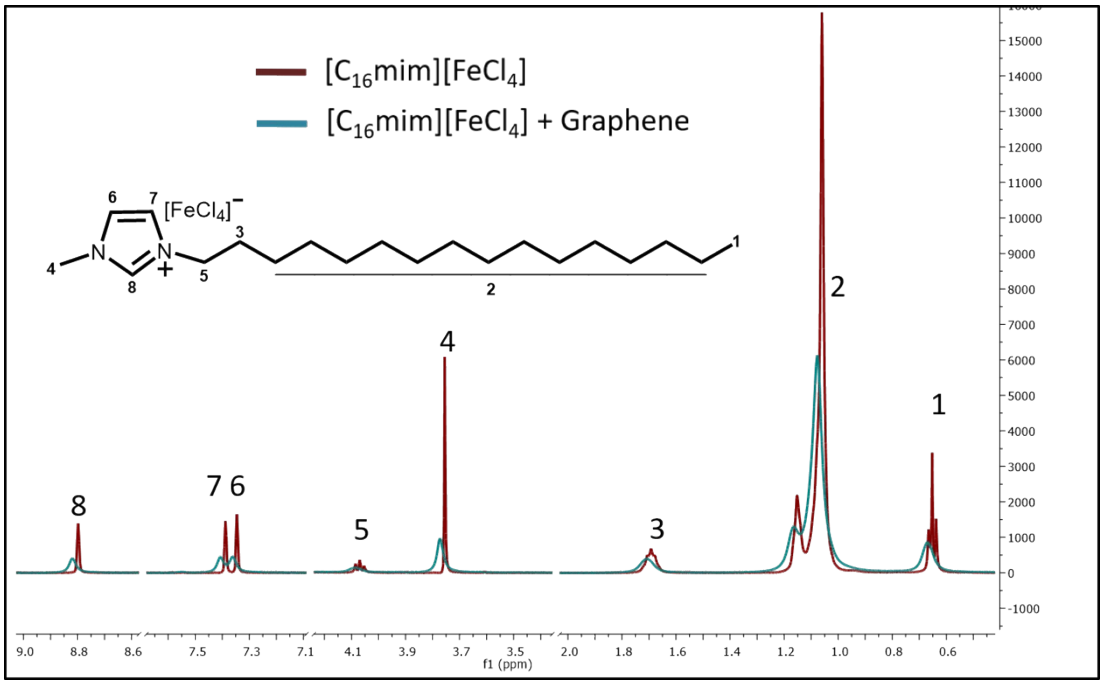

Figure S4: ^1H NMR of 5 mmol L^{-1} aqueous solution of $[C_{16}mim][FeCl_4]$ without graphene ($[C_{16}mim][FeCl_4]$ only) and with graphene ($[C_{16}mim][FeCl_4]$+ Graphene). The small downfield shift and broadening of peaks for different protons of $[C_{16}mim][FeCl_4]$ in the presence of graphene in comparison to $[C_{16}mim][FeCl_4]$ protons in the absence of graphene suggests the close proximity of protons $[C_{16}mim][FeCl_4]$ due to the interaction of hydrophobic part of $[C_{16}mim][FeCl_4]$ with graphene sheets.

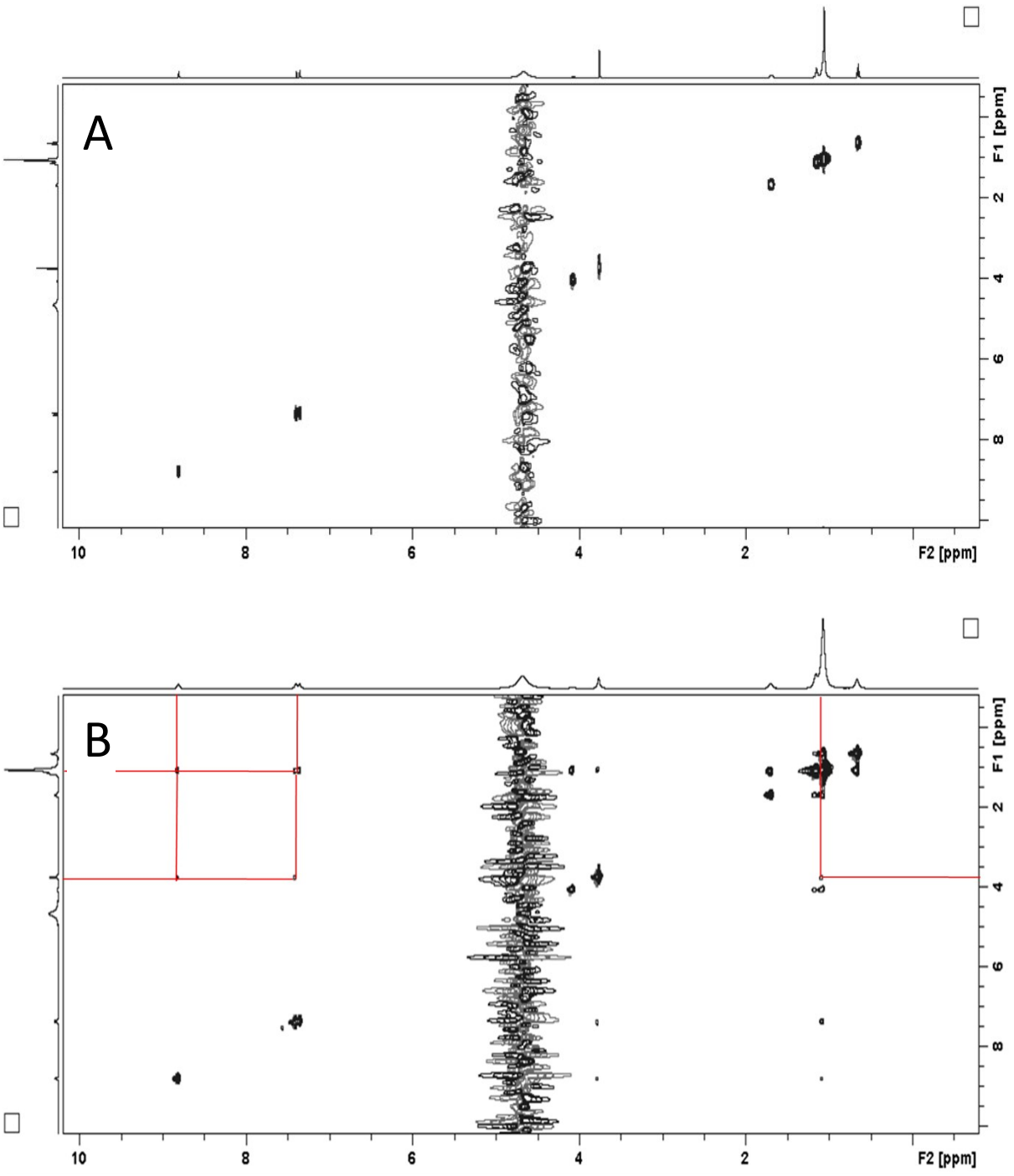

Figure S5: (A) 2D ^{1}H -^{1}H NOESY spectra of aqueous solution of [C_{16}mim][$FeCl_4$] in absence of graphene; (B) 2D ^{1}H-^{1}H NOESY spectra of aqueous [C_{16}mim][$FeCl_4$] in the presence of graphene. The appearance of correlation peaks in the presence of graphene indicates increase in through-space interactions between the protons of [C_{16}mim][$FeCl_4$] due to the adsorption of[C_{16}mim][$FeCl_4$] on graphene sheets.

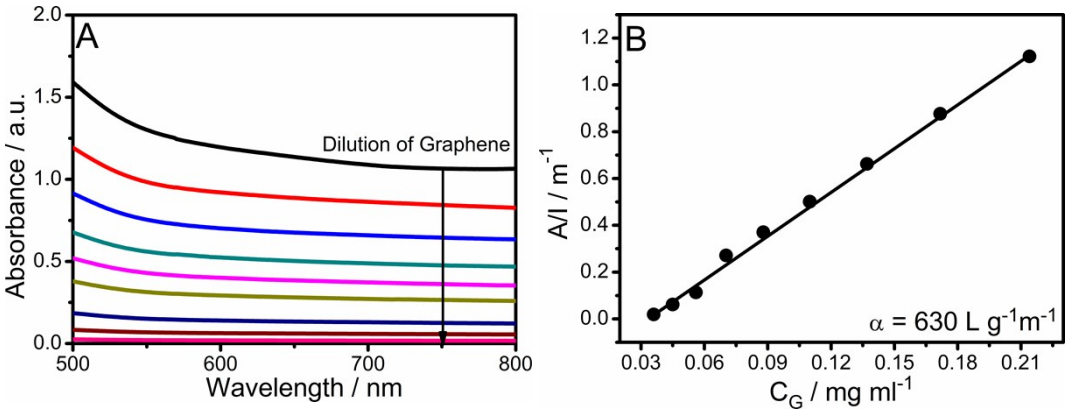

Figure S6: (A) Absorbance spectra of graphene at different concentrations; (B) Absorbance per unit length at 660 nm as a function of graphene concentration. The absorbance band for graphene is a flat and featureless band characteristic of graphene and other 2D materials.[10]

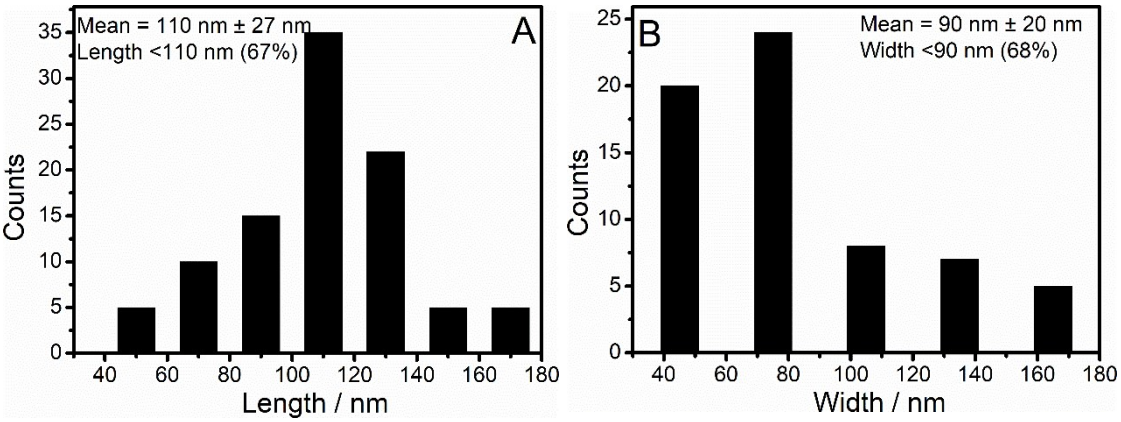

Figure S7: Statistical data obtained from analysis of AFM images of graphene sheets for (A) length and; (B) width. The number of the graphene sheets with length ≤ 110 nm are ≈ 67 % and with the width ≤ 90 nm are ≈ 68%.

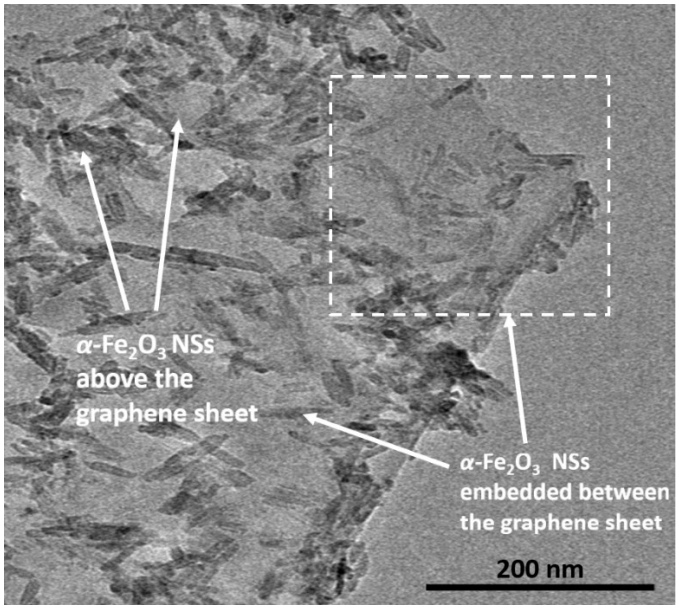

Figure S8: TEM image of α-Fe_2O_3@G showing α-Fe_2O_3NSs embedded between the graphene sheets and present above the graphene sheet.

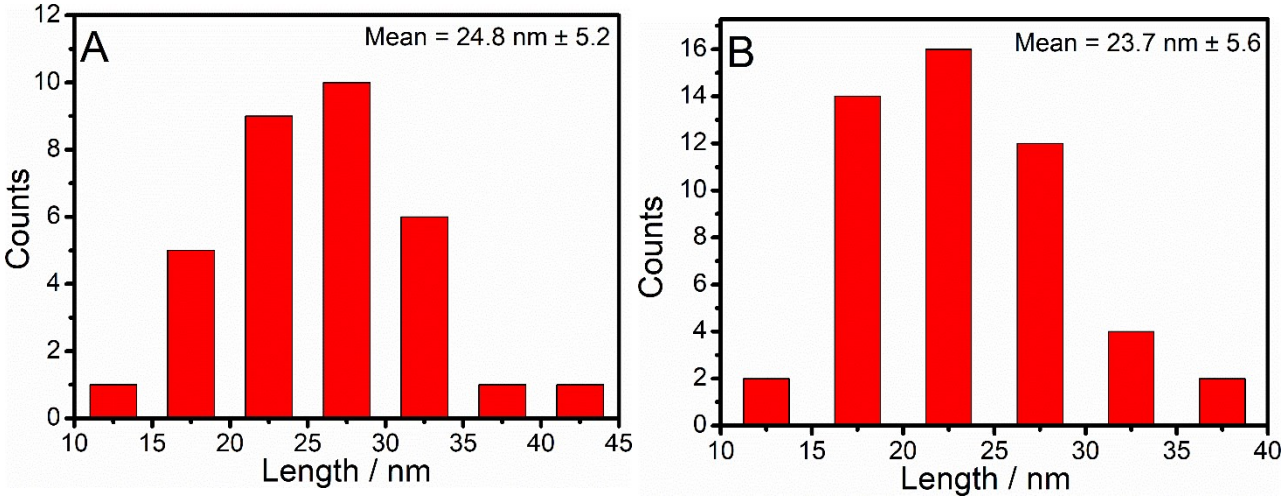

Figure S9: Histograms of length of prepared NSs (A) α-Fe_2O_3; (B) α-Fe_2O_3@G, showing no significant difference in the mean size of prepared NSs in the presence and absence of graphene.

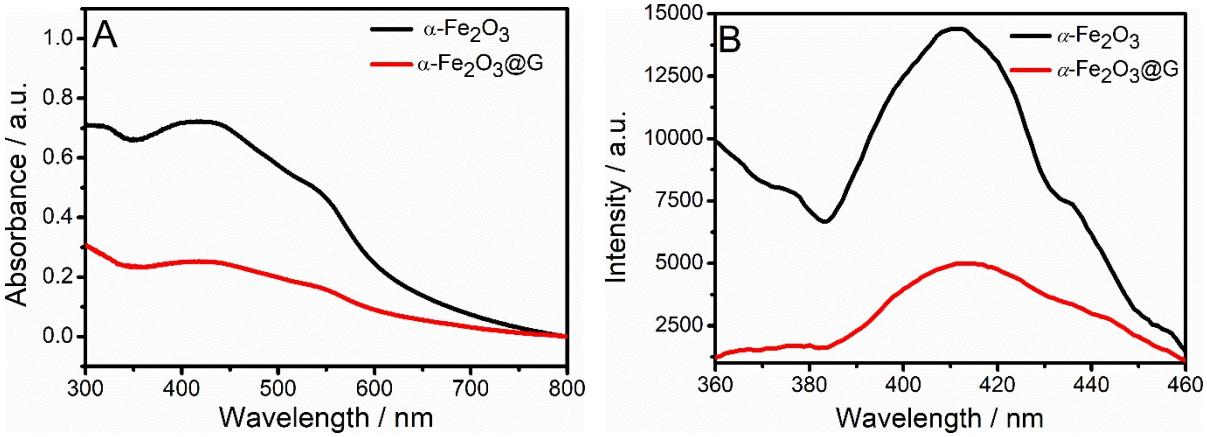

Figure S10: (A) UV-Vis and (B) Photoluminescence (PL) spectra of prepared α-Fe_2O_3@G composite and α-Fe_2O_3 by excitation at λ_{max}=320 nm.

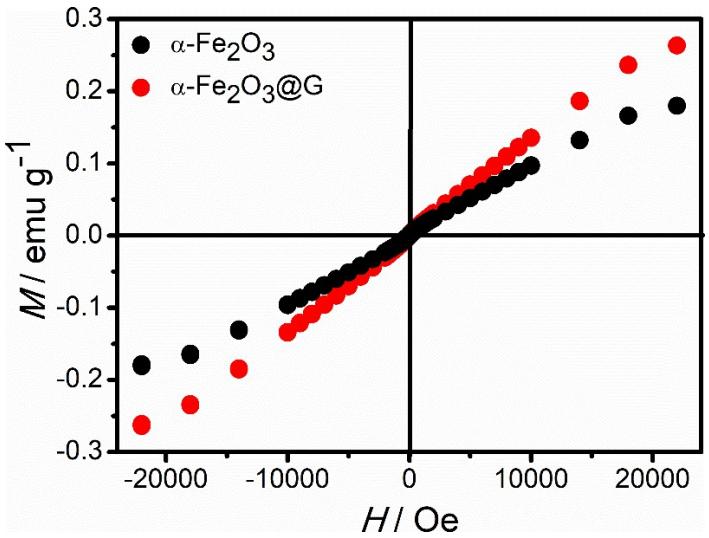

Figure S11: Hysteresis loop between applied field (M)-magnetic moment (H) of α-Fe_2O_3 NPs in the presence and absence of graphene sheets.

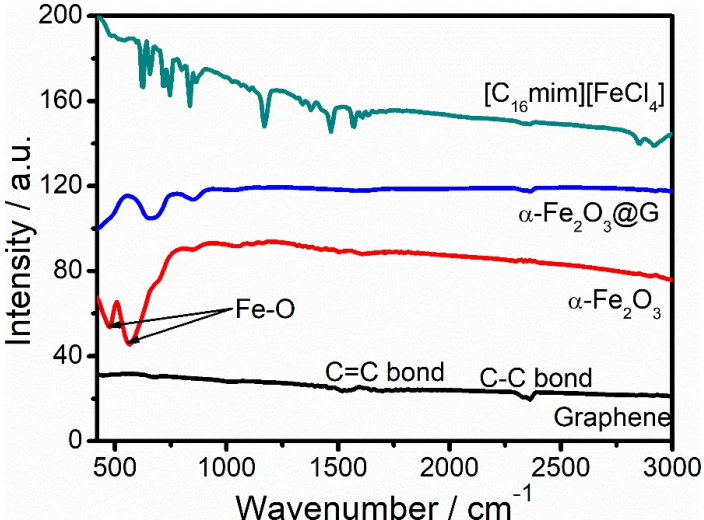

Figure S12: FT-IR spectra of preparedα-Fe_2O_3@G NCs, α-Fe_2O_3, Graphene, and $[C_{16}mim][FeCl_4]$.

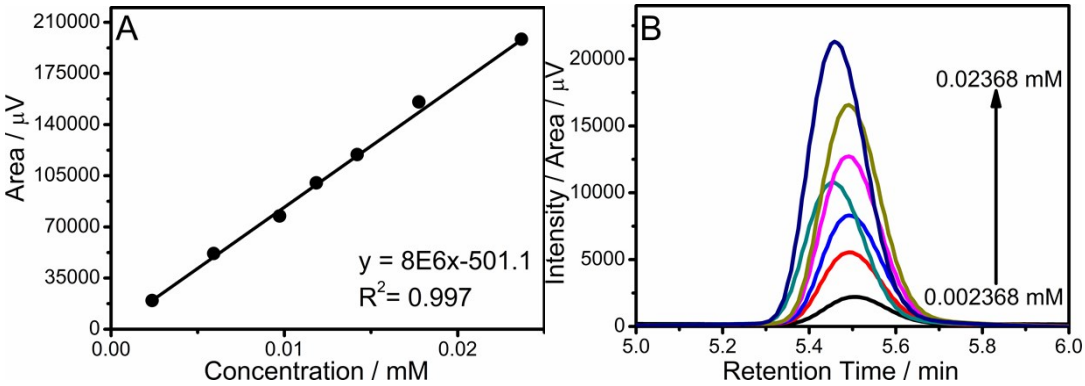

Figure S13: (A) Sulfamethoxazole (SMX) calibration and (B) HPLC calibration spectrum.

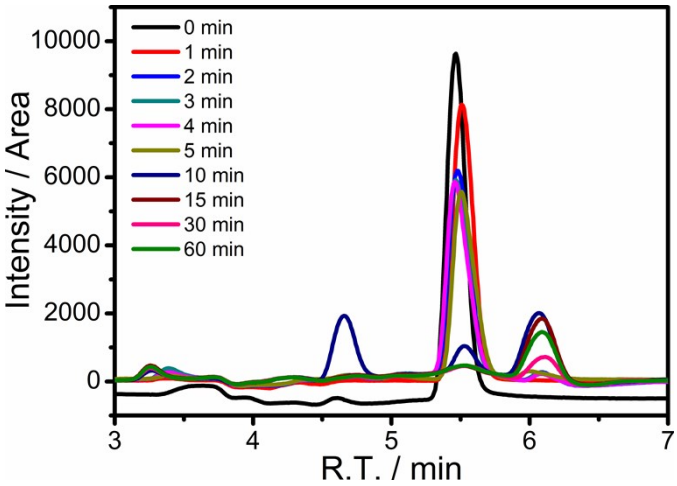

Figure S14: HPLC spectra of SMX at different time intervals upon addition of α-Fe_2O_3@G photo-catalyst.

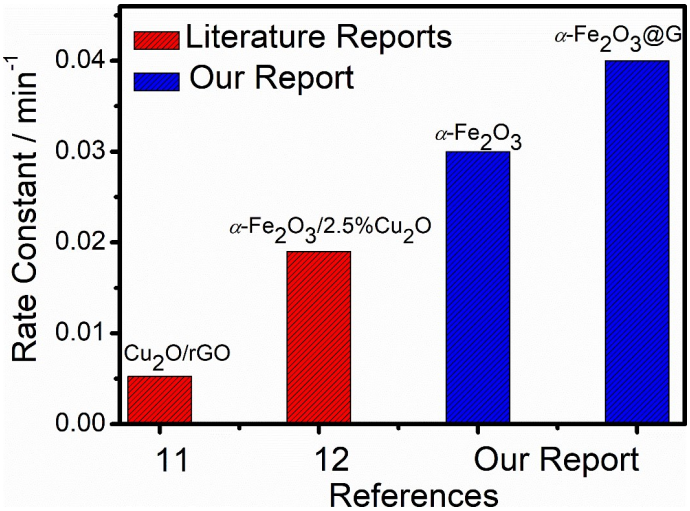

Figure S15: Comparison of rate constants of prepared photocatalyst with literature reports.[11-12]

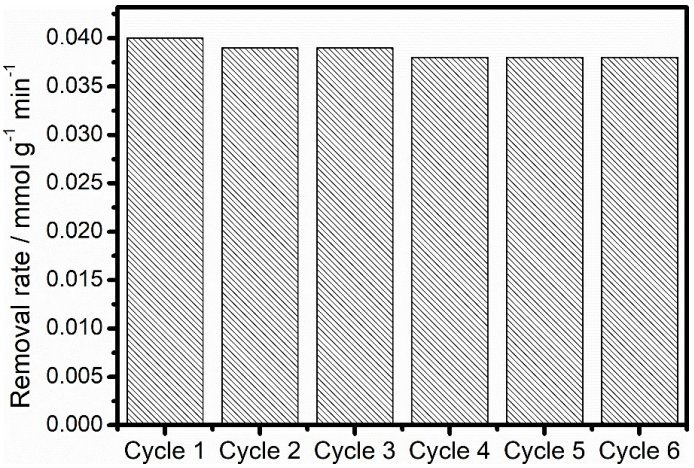

Figure S16: The photostability of prepared α-Fe_2O_3@Graphene photocatalyst upto 6 catalytic cycles.

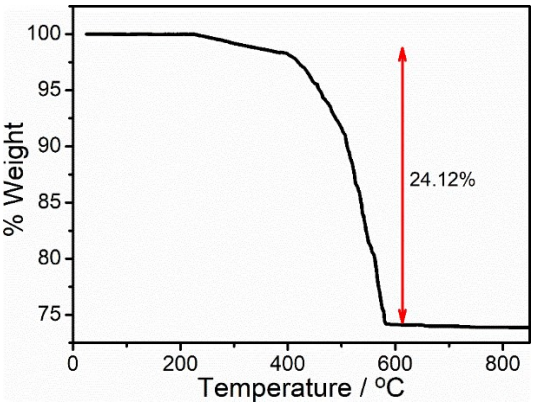

Figure S17: TGA measurement of prepared α-Fe_2O_3@G NCs. (24.12 % corresponds to graphene present in α-Fe_2O_3@G NCs and rest 75.8 % is α-Fe_2O_3)

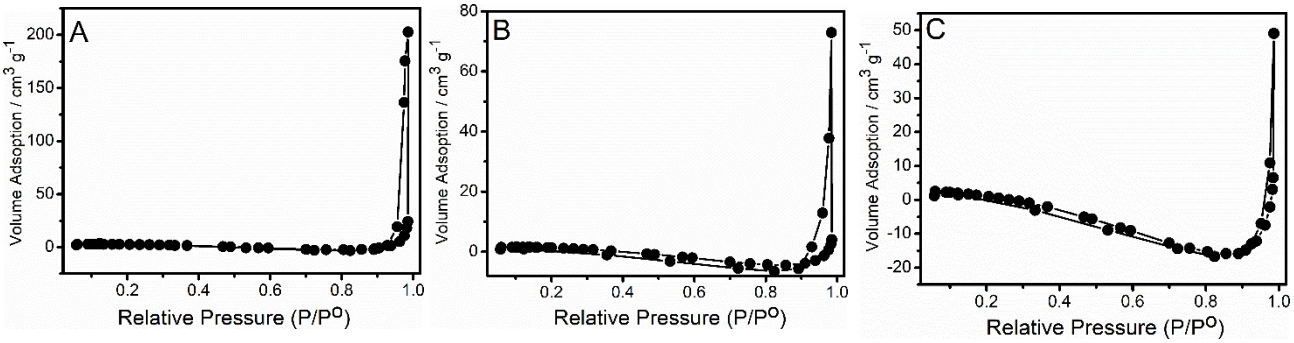

Figure S18: N_2 adsorption/desorption isotherms of (A) α-Fe_2O_3@G NCs; (B) α-Fe_2O_3; (C) Graphene.

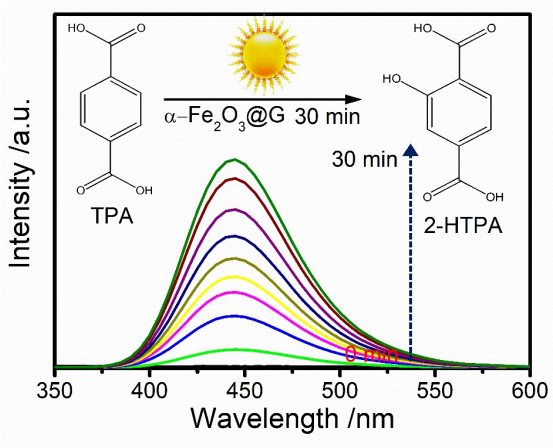

Figure S19: Hydroxyl radicals trapping over Fe_2O_3 @G by PL spectroscopy

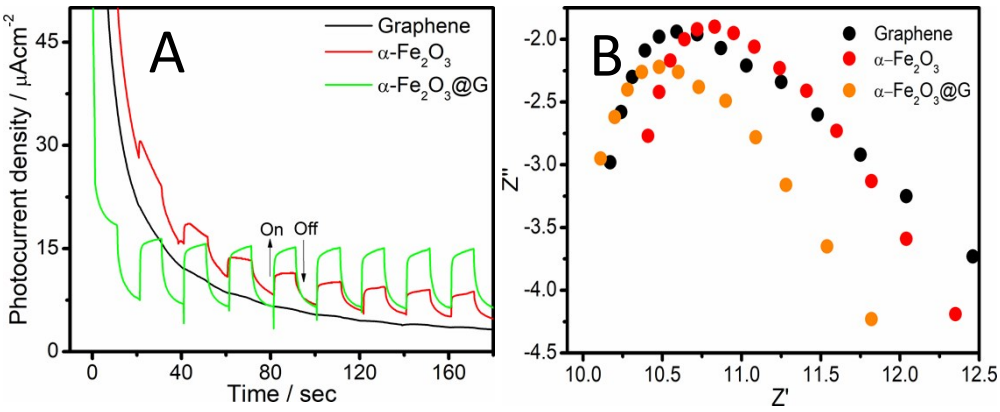

Figure S20: (A) Transient photocurrent; (B) EIS (Nyquist) plot at 0 V *vs*. RHE under illumination, of graphene, α-Fe_2O_3 and α-Fe_2O_3@G.

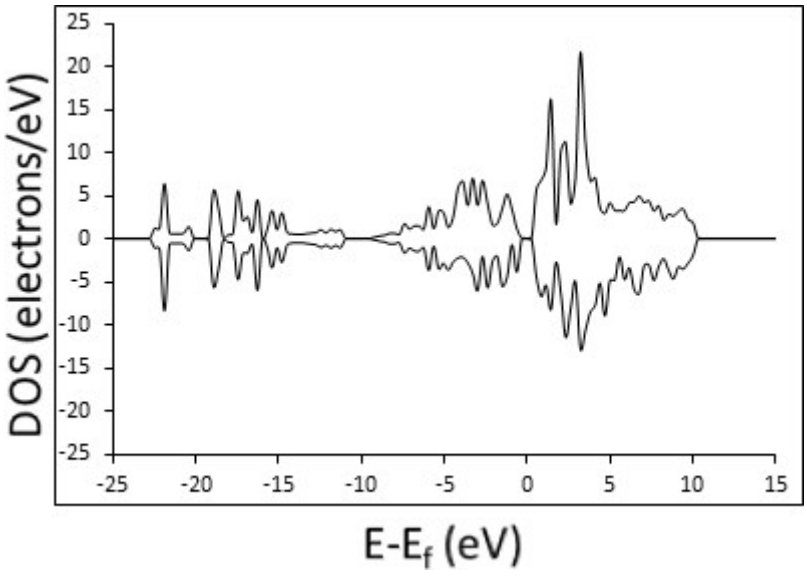

Figure S21: Total density of states (TDOS) of Fe_2O_3-A interfacial complex. Fermi level has been adjusted to zero. The graph above zero value indicates spin up and the graph below zero is spin down density of states.

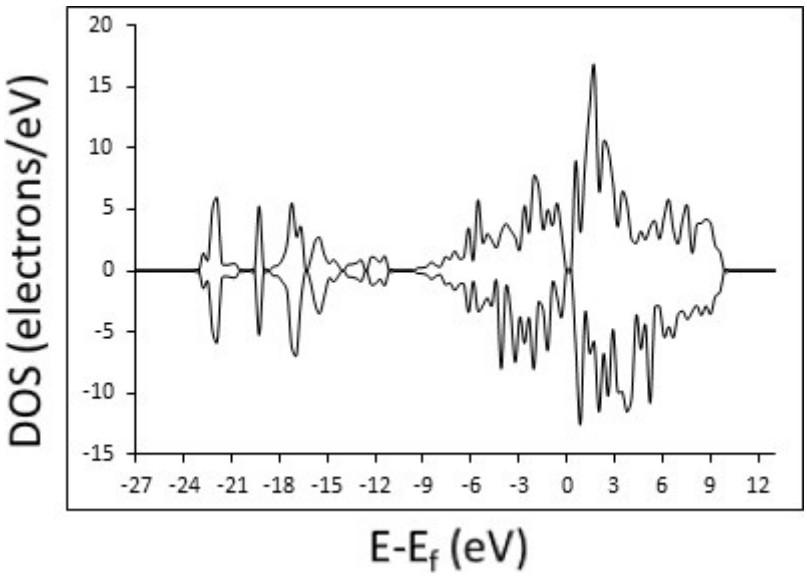

Figure S22: Total density of states (TDOS) of Fe_2O_3-B interfacial complex. Fermi level has been adjusted to zero. The graph above zero value indicates spin up and the graph below zero is spin down density of states.

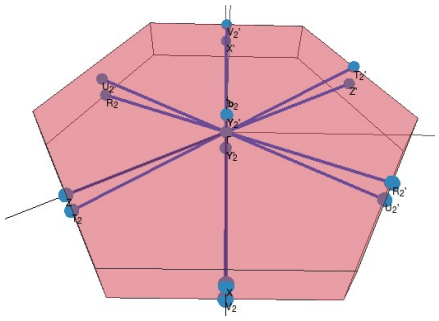

Figure S23: Representation of high symmetrical points around Γ-Centre as recommended by SeeK Path.

Table S1: Values of saturation magnetisation (M_s), remanent magnetisation (M_r) and coercivity (H_C) obtained from hysteresis loop for α-Fe_2O_3 NPs in the presence and absence of graphene sheets

Sample Code	α-Fe_2O_3	α-Fe_2O_3@G
M_r / emu/g	0.74×10^{-3}	0.87×10^{-3}
M_s/ emu/g	0.18	0.26
H_c / Oe	42.2	14.5

Table S2: The degradation kinetics and rate constants for the photodegradation of SMX by prepared photocatalyst.

Sample Code	Degradation kinetics	Rate constants / mmol g^{-1} min^{-1}
α-Fe_2O_3@G	92%	0.04
α-Fe_2O_3	59 %	0.03
Graphene	3.3%	0.0015
α-Fe_2O_3@reduced Graphene	69%	0.032

Table S3: The degradation kinetics and rate constants for the photodegradation of SMX by prepared photocatalyst.

Sample Code	Surface Area / m^2/g	Pore Size / nm
α-Fe_2O_3@G	84.8	13.2
α-Fe_2O_3	29.5	3.6
Graphene	44.5	6.5

References

1. (a) F. G. Sherif, L. J. Shyu, and C. C. Greco, U.S. Patent, 5,824, 832 (1998). 25. (b) Q. F. Yue, H. G. Yang, M. L. Zhang, and X. F. Bai, *Adv. Mater. Sci. Eng.*, 2014, 454756. (c) Komal, H. Kaur, M. Kainth, S. S. Meena and T. S. Kang. *RSC Adv*., 2019, **9**, 41803-41810.
2. D. Nuvoli, L. Valentini, V. Alzari, S. Scognamillo, S. Bittolo Bon, M. Piccinini, J. Illescas and A. Mariani, *J. Mater. Chem*., 2011, **21**, 3428-3431.
3. J. P. Perdew, K. Burke and M. Ernzerh, *Phys. Rev. Lett.*1996, **77**, 3865–3868.
4. D. Joubert, *Phys. Rev. B:Condens. Matter Mater. Phys.*1999, **59**, 1758–1775.
5. H. J. Monkhorst and J. D. Pack, *Phys. Rev. B: Solid State*1976, **13**, 5188–5192.
6. G. Kresse and J. Hafner, *Phys. Rev.B: Condens. Matter Mater. Phys*. 1993, **47**, 558–561.
7. G. Kresse, J. Furthmuller, *Phys. Rev. B: Condens. Matter Mater. Phys.*1996, **54**, 11169–11186.
8. G. Kresse, J. Hafner, *Phys. Rev. B: Condens. Matter Mater. Phys.*1994, **49**, 14251–14269.
9. Materials Project, http://www.materialsproject.org.
10. D. S. L. Abergel and V. I. Fal'ko, *Phys. ReV. B* 2007, **75**, 155430-155435.
11. S.-H. Liu, Y.-S. Wei and J.-S. Lu, *Chemosphere*, 2016, **154**, 118-123.
12. Y. Feng, C. Liao, H. Li, C. Liu and K. Shih, *Environ. Technol*., 2018, **39**.